Targeting Schwann cells by nonlytic arenaviral infection selectively inhibits myelination

Anura Rambukkana*†, Stefan Kunz‡, Jenny Min*, Kevin P. Campbell§, and Michael B. A. Oldstone‡

*Laboratory of Bacterial Pathogenesis and Immunology, The Rockefeller University, New York, NY10021; ‡Division of Virology, Department of Neuropharmacology, The Scripps Research Institute, La Jolla, CA 92037; and §Howard Hughes Medical Institute, and Departments of Physiology and Biophysics and Neurology, University of Iowa, Iowa City, IA 52242-1101

Members of the arenavirus family, famous for their hemorrhagic syndromes, cause distinct neurological disorders; however, cellular and molecular targets as well as pathogenesis of peripheral nervous system disorders associated with these viruses are unknown. Using noncytolytic lymphocytic choriomeningitis virus, the prototype arenavirus, and pseudotyped Lassa fever virus, we showed that the Schwann cells, but not the neurons, were preferentially targeted and harbored the virus. This permissiveness was caused by the viral glycoprotein usage of its receptor α-dystroglycan, which was highly abundant on Schwann cell membranes. Persistent lymphocytic choriomeningitis virus infection rendered immature Schwann cells defective or incapable of forming compact myelin sheathes when they differentiated to myelinating phenotype in an in vitro differentiation model of Schwann cells. Persistent infection did not cause Schwann cell apoptosis or cytopathic effect. Defects in myelination coincided with the down-regulation of dystroglycan expression and disruption of the laminin-2 organization and basal lamina assembly on Schwann cell-axon units. The data provide evidence for a selective perturbation of laminin-2–laminin-2 receptor communication pathway in the peripheral nervous system by a nonlytic virus and the resulting myelin defects, which may partly contribute to neurological abnormalities associated with arenaviral infection.

T he members of the arenavirus family, famous for their hemorrhagic syndromes in humans (1), are also linked to distinct neurological disorders of both central and peripheral nervous systems (2–9). Among the arenaviruses, Lassa fever virus (LFV) and lymphocytic choriomeningitis virus (LCMV) have been shown to cause neurological abnormalities (2–9). However, neurological damage and neuropathogenesis caused by arenaviral infections are largely unknown, because most of the studies have focused on the deadly hemorrhagic syndromes, which have contributed to high mortality rate (10, 11). In the case of the peripheral nervous system (PNS), no experimental data are available to evaluate the involvement of the PNS and associated neuropathogenesis in LFV or LCMV infections. Thus, nothing is known about the cellular and molecular targets of arenaviruses in the PNS. Moreover, recent studies have underscored the need for further research in congenital infection with LCMV in human, because LCMV is considered as underdiagnosed fetal teratogen (9). Importantly, congenital LCMV infection may also affect the developing nervous system in human fetus, which could lead to lasting neurophysiologic abnormalities in infants and children (9).

Despite the severity of infection, arenaviruses actually cause very little damage to the infected tissues. At any rate of infection, cells exhibit little virus-induced cytopathy (10–13). Thus, a candidate mechanism for arenavirus-induced disease is through functional effects of the viruses that are not associated with overt evidence of cellular damage. Indeed, it has been shown that persistent infection with LCMV interferes with differentiated functions of the host cells without incurring structural injury (12, 13). For this reason, noncytolytic viruses such as LCMV may serve as an excellent model for studying how they interfere with specific nerve cell functions. Among the arenaviruses, the best studied is the LCMV whose genome consists of two segments of single-stranded RNA, each coding for two genes by using an ambisense strategy of replication (reviewed in ref. 14). The larger segment encodes the virus polymerase and a small zinc finger motif protein, and the smaller segment encodes the virus nuclear protein (NP) and glycoprotein (GP) precursor, which is posttranslationally cleaved into GP1 and GP2. GP-1 anchors LCMV and LFV to host cell surface through a recently identified viral receptor, α-dystroglycan (15–18).

Dystroglycan, a major laminin receptor originally identified in muscles complex with dystrophin, is encoded by a single gene and cleaved into two proteins, α- and β-dystroglycan by posttranslational processing (19). α-Dystroglycan is also identified as a major laminin-2 and agrin receptor in Schwann cells of the PNS (20). Dynamic interactions of dystroglycan with the components of the extracellular matrix (ECM), particularly laminins, are integral to tissue morphogenesis. This was illustrated by the recent findings that genetic or functional ablation of dystroglycan and other laminin receptors disrupt the process of laminin assembly and alter laminin expression on the cell surface (21, 22). Similarly, dystroglycan appears to play a critical role in the assembly of laminin-2-rich basal lamina on Schwann cell-axon units and in maintaining the architecture of sodium-ion channels, and thus proper nerve conduction (20, 23, 24). In the PNS, Schwann cells are responsible for the secretion of matrix components and assemble them into an organized basal lamina around Schwann cell-axon units (25–27). Several lines of evidence implicate the role of laminin-2, a heterotrimer consisting of α2, β1, and γ1 chain subunits, and the major ECM molecule of the Schwann cell basal lamina, in myelination (27–30). These findings together with high-affinity binding of α-dystroglycan to laminin-2 (31) suggest the potential role of Schwann cell dystroglycan in laminin-2-mediated biological effects in the PNS. In the present study, we provided evidence that LCMV, by specifically targeting α-dystroglycan on Schwann cells, interfered with the laminin–dystroglycan communication system in the PNS and perturbed the myelination process.

Experimental Procedures

Virus Strains, Virus Purification, and Virus Quantification. *LCMV strains.* LCMV Armstrong ARM53b and LCMV cl13 are viruses whose origin, structure, and function have been reported (16, 32, 33). Seed stocks of all viruses were prepared by growth in BHK-21 cells, and viral titers were determined as described (32, 33). LFV was inactivated and obtained from the Centers for Disease Control and Prevention (Atlanta) by using 5×10^6 rad γ-irradiation.
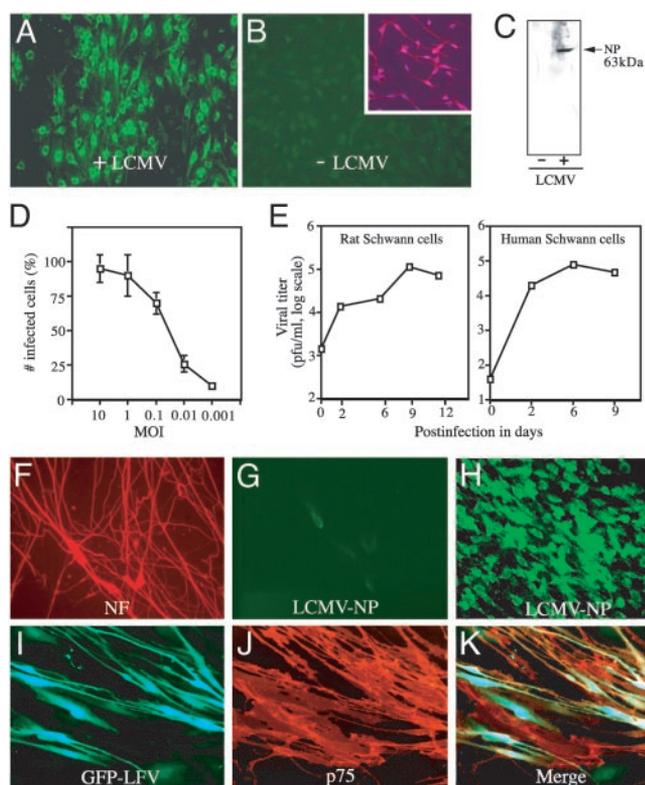*Generation of GFP-LFV-PS.* Moloney murine leukemia virus (MLV) virions containing LFVGP at their surface (LFV-PS) were generated by using the strategy reported by Soneoka *et al.* (34) and are

Fig. 1. Schwann cell is the preferential PNS target for LCMV and LFV. (*A–E*) LCMV strain cl-13 avidly infects and replicates in primary rat and human Schwann cells. Labeling of infected (+LCMV) (*A*) and uninfected (−LCMV) (*B*) Schwann cells with mAb 1-1-3 specific for LCMV-NP. (*Inset*) The purity of primary Schwann cells; all nucleated cells were positive for antibody to S-100. (*C*) Immunoblots of infected (+) and noninfected (−) Schwann cell lysates were labeled with mAb 1-1-3, depicting the 63-kDa NP of LCMV only in infected cultures. (*D*) Quantification of LCMV-infected Schwann cells using different mois of virus. (*E*) Replication of LCMV cl-13 in rat (*Left*) and human (*Right*) Schwann cells. (*F–H*) DRG neurons are resistant to LCMV infection. Purified DRG neurons infected with LCMV cl-13 were fixed after 18 h as in *A* and double-labeled with antibodies to neurofilament (NF) (*F*) and LCMV-NP (*G*), showing no detectable viral antigens in neurons. (*H*) DRG neurons (as in *F*) that are cocultured with Schwann cells for 3 weeks were infected with LCMV and labeled with mAb 1-1-3 to show viral detection only in Schwann cells. (*J–K*) Primary human Schwann cells are susceptible to pseudotyped LFV. Purified human Schwann cells (shown in *J* as labeled with Schwann cell-specific anti-p75 mAb) infected with GFP-MLV virions containing LFV-GP on their surface (LFV-PS) were infected at a moi of 1. (*I*) GFP-expressing cells denote the specific Schwann cell infection via LFV-GP. (*K*) Colocalization of LFV-GP-positive cells with anti-p75 is shown in the merge image. (Magnifications: ×40.)

described in *Supporting Text*, which is published as supporting information on the PNAS web site.

Primary Cultures of the PNS. Preparation of dorsal root ganglia (DRG), primary rat Schwann cell and DRG neuron cultures, myelinating Schwann cell-neuron cocultures, and primary human Schwann cells was done according to established protocols (35–38) and as described in *Supporting Text*.

Viral Infection of Primary PNS Cultures. Embryonic DRG explant cultures were infected with LCMV cl-13 at a multiplicity of infection (moi) of 3 and maintained in C media for 3 days before the addition of ascorbic acid to promote basal lamina assembly and myelination. In parallel, control cultures were maintained under similar conditions, but without virus. Cultures were processed at different time intervals (up to 21 days) for immunofluorescence, immunoblotting, and electron microscopy as described (37, 39). These cultures were

also processed for BrdUrd uptake with a BrdUrd assay kit and a terminal deoxynucleotidyltransferase-mediated dUTP nick end labeling assay kit (Roche Molecular Biochemicals) (37). Infection of primary rat Schwann cells and neurons and infection of human Schwann cells with MLV virions pseudotyped with LFVGP are described in *Supporting Text*.

Preparation of α-Dystroglycan from Human Peripheral Nerves and Primary Schwann Cells. α-Dystroglycan was purified from human peripheral nerve tissue and primary rat and human Schwann cell cultures as well as skeletal muscles according to previously established protocols (19) and as described in *Supporting Text*.

Antibodies. All primary monoclonal and polyclonal antibodies used in this study are described in *Supporting Text*.

Quantitation of Myelination. Total numbers of myelin segments were quantified (37) and are described in *Supporting Text*.

Assays for Virus Binding to Schwann Cell Dystroglycans. Virus overlay protein binding assay (VOPBA) using purified LCMV and LFV was performed as described (15–17) and as described in *Supporting Text*.

Inhibition of Virus Binding to α-Dystroglycan by Laminin-2. Blocking of virus binding by laminin-2/α2 laminins (merosin) in VOPBA was carried out as described (17). ELISA was used to measure laminin-2 competition for the binding of LCMV to α-dystroglycan. Both inhibition assays are described in *Supporting Text*.

Results

Schwann Cell Serves as the Preferential PNS Target for LCMV and LFV. To determine the cellular and molecular target of the PNS for LCMV and LFV, we used different *ex vivo*-type primary nerve tissue culture models in which each component of the PNS was studied individually or in combination for their susceptibility. They consisted of both human and rat primary culture systems: (*i*) human Schwann cells isolated and purified from one human donor, (*ii*) purified rat primary Schwann cells, (*iii*) DRG neurons, (*iv*) myelinating DRG explant cultures consisting of Schwann cells, neurons, and fibroblasts, and (*v*) purified Schwann cell-neuron cocultures with myelinating and nonmyelinating axons. Infection of LCMV clone-13 (cl-13) with the above-mentioned primary rat peripheral nerve cultures indicated that LCMV avidly infected only the Schwann cells. This finding was confirmed by the LCMV infection of highly purified (100%) primary rat Schwann cells in a dose-dependent manner (Fig. 1 *A–C*). In infected Schwann cells, LCMV NP antigens could easily be detected in fixed cells and whole-cell lysates by using specific mAb 1-1-3 to LCMV-NP (Fig. 1 *A* and *B*). One moi of LCMV [1.5×10^4 plaque-forming units (pfu) per well] resulted in >90% Schwann cell infectivity (Fig. 1 *A–D*). Also, Schwann cells provide a suitable target for LCMV replication, as viral titers as high as $>1 \times 10^6$ pfu/ml could be detected 9–10 days after infection (Fig. 1*E Left*). Identical results were obtained from LCMV infection of human Schwann cells (Fig. 1*E Right* and data not shown). Despite replication, LCMV did not cause any morphological alteration or cytopathic effect to rat or human Schwann cells. Double immunolabeling of mixed nerve cultures with Schwann cell-specific antibodies to S-100 or p75 (low-affinity nerve growth factor receptor) and mAb 1-1-3 (15) further revealed preferential LCMV infection in Schwann cells (Fig. 1*H* and data not shown). In contrast, purified DRG neurons were not infected by LCMV (Fig. 1 *F* and *G*).

We next cocultured purified DRG neurons with purified rat Schwann cells and allowed them to ensheath and myelinate for 3–4 weeks. These cocultures contain both myelinated and nonmyelinated Schwann cell phenotypes in the form of Schwann cell-axon units as in *in vivo* (39). LCMV infection could be detected in both

myelinated and nonmyelinated Schwann cells with no phenotypic preference, but not in the enclosed axons (Fig. 1 *G* and *H*). Because LCMV replicates nonlytically and efficiently within rat and human Schwann cells, Schwann cells possess crucial host factors necessary for viral replication and thus serve as reservoirs for LCMV in the PNS.

To determine whether these findings hold true for LFV infection, we used highly purified human Schwann cells at early passages (passage 3) in primary cultures (Fig. 1*J*). Because initial LFV interaction with host cell is mediated by the LFV surface GP (15, 18), we generated MLV containing GFP transgene pseudotyped with LFV-GP for infection of human Schwann cells. Because of its infectious nature and high mortality rates, the use of infectious LFV is restricted. The use of LFV-GP pseudotyped virus (LFV-PS) partly solved the problem, enabling analysis of cell binding and entry of LFV to target cells. At a LFV-PS concentration of 1 moi, 31.5% (±4.1 SD) of human Schwann cells were found infected with LFV-PS as determined by GFP-positive cells (Fig. 1 *I–K*). The negative control, the GFP-MLV virions that lack LFV-GP construct, showed no GFP-positive cells (data not shown), indicating that human Schwann cell infection is mediated by LFV-GP. Infectivity of LFV-PS in primary human Schwann cells suggest that Schwann cells are the likely PNS target in natural LFV infection in human.

Schwann Cell Entry of LCMV and LFV Is Mediated by α-Dystroglycan. To determine the viral receptor on Schwann cells, we used VOPBA (15, 17) with membrane fractions of primary rat and human Schwann cells and human peripheral nerves. Both LCMV cl-13 and LFV strongly bound to a single protein band with broad migration pattern at a molecular mass of $\approx$120 kDa. This protein was migrated in a similar molecular size as purified α-dystroglycan (Fig. 2*A* and *B*), a previously identified cell receptor for LCMV and LFV (15). Purified soluble α-dystroglycan (Fig. 2*G*) dramatically inhibited LCMV infection of primary rat Schwann cells in a dose-dependent manner (Fig. 2 *C–F*), suggesting that α-dystroglycan is responsible for LCMV infection of Schwann cells. High infectivity of LCMV is probably caused by the presence of α-dystroglycan in high density on the peripheral membrane of primary Schwann cells (Fig. 2*E*) (36). We could not detect α-dystroglycan on purified DRG neurons in primary cultures (data not shown). This finding parallels the resistance of DRG neurons to LCMV and LFV infections. Similarly, strong binding of LFV to α-dystroglycan from human peripheral nerves and human Schwann cells (Fig. 2*B*) suggests that human PNS infection by LFV is mediated by Schwann cell α-dystroglycan.

LCMV Infection Down-Regulates α-Dystroglycan Expression in an *in Vitro* Model of Schwann Cell Differentiation. To delineate the functional effects of LCMV infection of Schwann cells, we infected immature Schwann cells in DRG explant cultures from embryonic day 16 rat embryos. LCMV infection (moi 3) of 5-day-old DRG explant cultures (Fig. 3*A*) produced 100% infection exclusively in Schwann cells as LCMV-NP antigen was detected in all S-100-positive Schwann cells (Fig. 3 *B* and *C*). We then allowed Schwann cells to differentiate fully and studied the effects of LCMV infection in major Schwann cell functions, ECM production, basal lamina assembly, and myelination.

Analyzing LCMV-infected cultures after induction of myelination at different time intervals reveals that viral infection dramatically down-regulated the expression of α-dystroglycan on Schwann cells (Fig. 3 *H* and *I*) at day 10 postinfection. Strikingly, the down-regulation of α-dystroglycan was confined mainly to Schwann cells that are ensheathing axons or Schwann cell-axon units, but not to the ganglion areas (Fig. 3 *H* and *G*). In control cultures, the expression of α-dystroglycan on myelinated fibers could be seen as discrete tubular appearance (Fig. 3 *E* and *F*), whereas in infected cultures labeling was detected only in a few individual Schwann cells
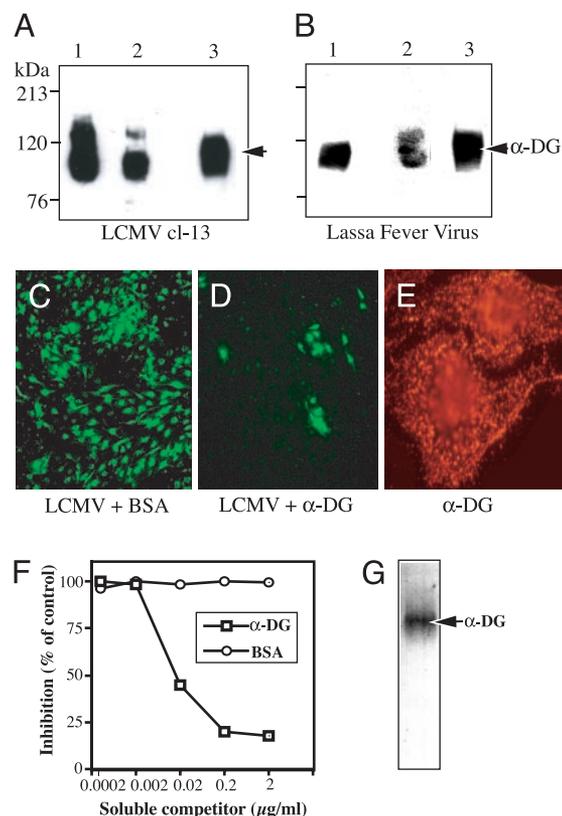
Fig. 2. Neural permissiveness of LCMV and LFV is caused by the viral usage of α-dystroglycan (α-DG) receptor on Schwann cells. (*A* and *B*) Identification of LCMV and LFV receptors on Schwann cells. VOPBA with mAb that recognize identical peptide epitopes of GP1/2 of LCMV and LFV showing the binding of LCMV cl-13 (10^7 pfu/ml) (*A*) and LFV (10^8 pfu/ml) (*B*) to the blots of primary rat and human Schwann cells and human peripheral nerve membrane fraction. (*A*) LCMV-bound proteins are from total lysates of primary rat Schwann cells (lane 1), membrane fraction of rat Schwann cells (lane 2), and purified α-dystrolycan from skeletal muscles as a positive control (lane 3). (*B*) LFV-bound proteins are from human peripheral nerve membrane fraction (lane 1), membrane fraction of primary human Schwann cells (lane 2), and purified α-dystrolycan (lane 3). (*C–G*) Blocking of LCMV infection of primary Schwann cells by soluble α-dystrolycan. Primary rat Schwann cells were infected with LCMV cl-13 at a moi of 0.1 in the presence of BSA (*C*) and soluble α-dystrolycan (*D*), and the viral antigens were detected by mAb 1-1-3. (*E*) Abundance of α-dystrolycan on live primary rat Schwann cells as detected by anti-α-dystrolycan mAb IIH6. (*F*) Quantification of percent inhibition of LCMV infection of Schwann cells by increasing concentration of soluble α-dystrolycan as in *C* and *D*. Note the dramatic decrease of LCMV entry by soluble α-dystrolycan. (*G*) Commassie blue-stained gel showing the purity of α-dystrolycan used in inhibition studies and as positive controls in *A* and *B*. (Magnifications: ×40.)

(Fig. 3 *H* and *I*). Although less prominent, the pattern of β-dystroglycan expression in infected cultures was almost similar to α-dystroglycan (data not shown). However, we found no difference in the expression of Dp116 and actin filament labeling, although β-dystroglycan is known to bind to Dp116 in Schwann cells (30). Also, no significant difference was observed in the expression of other laminin-2 receptors such as β1 and β4 integrins in infected and control cultures (data not shown). Moreover, studies by electron microscopy, as well as BrdUrd uptake and terminal deoxynucleotidyltransferase-mediated dUTP nick end labeling assays at different time points, revealed that LCMV, as compared with control, does not affect Schwann cell ensheathment, proliferation, or cell death, respectively (Fig. 4 *F* and *H* and data not shown).

Immature Schwann Cells Persistently Infected with LCMV Disrupt the Organization of Laminin-2 Network on Schwann Cell-Axon Units. We next examined whether LCMV-induced α-dystroglycan modulation

NEUROSCIENCE
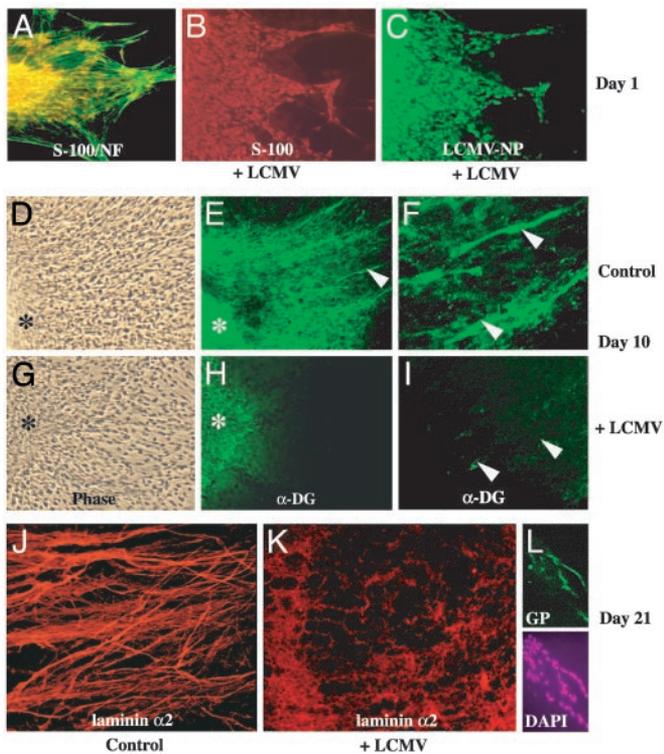
Fig. 3. LCMV infection of immature Schwann cells down-regulates α-dystroglycan expression and ablates laminin-2 assembly: A time course study. (*A–C*) LCMV infection in immature Schwann cells. (*A*) DRG explant cultures from embryonic day 16 rat embryos that are maintained in for 5 days are double-labeled with antibodies to S-100 and neurofilaments (NF) to show the position of Schwann cells (red/yellow) and neurite outgrowths (green), respectively. At day 5, these cultures were also positive for α-dystroglycan (data not shown). Parallel cultures were infected with LCMV cl-13 and double-labeled with antibodies to S-100 (*B*) and LCMV-NP (*C*). Note that viral antigens are present in all S-100-positive cells (*B* and *C*), and LCMV–NP was not detected in neurite outgrowths. (*D–I*) Immature Schwann cells infected with LCMV show significant down-regulation of α-dystroglycan expression during differentiation. Infected (*E* and *F*) and noninfected (*H* and *I*) explant cultures were labeled with mAb IIH6 specific for α-dystroglycan after 10 days. Note the absence or weak expression of α-dystroglycan specifically on infected Schwann cells that are ensheathing axons or on Schwann cell-axon units (*H* and *I*) but not in the ganglion area (shown by ∗). Corresponding phase-contrast images of *E* and *H* are shown in *D* and *G*, respectively. Higher magnification in *F* shows the α-dystroglycan on myelinated fibers (arrowheads), whereas in infected cultures, α-dystroglycan expression is confined to a few individual Schwann cells (*I*, arrowheads). (*J* and *K*) Disruption of the organization of laminin-2 network on Schwann cell-axon units during differentiation of LCMV-infected immature Schwann cells to mature phenotypes. Explant cultures were fixed 21 days after infection and labeled with antibody specific for laminin α2 chain. Note the disorganized laminin-2 network in infected cultures (*K*), whereas in controls, laminin α2 expression is uninterrupted along the nerve fibers and demarcate each fiber in a well-organized manner (*J*). (*L*) Similar cultures as in *K* were labeled with a mixture of mAbs against LCMV-GP1 and GP2 to show the expression of viral GP on Schwann cell-axon units (*Upper*). (*Lower*) Shown is 4′,6-diamidino-2-phenylindole (DAPI) labeling of Schwann cell nuclei in corresponding nerve fibers. (Magnifications: ×40.)

affects the assembly of basal lamina on Schwann cell-axon units. We used antibodies specific for the α2 chain as a marker for Schwann cell basal lamina (39). In control cultures, we found that laminin α2 labeling was uninterrupted and expressed in the form of thread-like fibers representing well-organized basal laminae on myelinated nerve fibers (Fig. 3*J*) (39). Strikingly, as compared with uninfected cultures, LCMV-infected immature Schwann cells that have differentiated to myelinated and nonmyelinated fibers after 21 days showed completely disorganized laminin-2 network with no demarcation of nerve fibers by laminin α2 (Fig. 3 *J* and *K*). However,

LCMV infection does not appear to affect the synthesis of laminin-2, because there was no difference in the intensity of laminin α2 labeling in both immunofluorescence (Fig. 3 *J* and *K*) and immunoblotting of total lysates of similar cultures (data not shown). Parallel studies with electron microscopy were in agreement with the data shown by immunolabeling and revealed disrupted basal lamina adjacent to the Schwann cell membrane in LCMV-infected cultures (Fig. 4*K*). In contrast, Schwann cell-axon units in control cultures showed continuous electron-dense layers that correspond to *lamina densa*, the typical ultrastructural morphology of the basal lamina (Fig. 4*J*). Because viral GP binds α-dystroglycan with high affinity (17, 18), LCMV-GP alone could contribute to perturbation of laminin-2 network and basal lamina assembly. The data shown in Fig. 3*L* illustrate the expression of LCMV-GP on Schwann cell-axon units in persistently infected cultures, suggesting such possibility.

Persistent LCMV Infection Selectively Inhibits Schwann Cell Myelination. In embryonic DRG explant cultures that mimic, in part, differentiation stages of Schwann cells *in vivo* (40), the promyelinating Schwann cells, that are ensheathing larger caliber axons in 1:1 relationship, subsequently form fully developed compact myelin sheath (Fig. 4 *A* and *G*). Strikingly, persistent LCMV infection not only inhibited this myelination process but also produced defective myelin sheaths, a condition similar to hypomyelination (Fig. 4 *D* and *H*). The total number of myelin segments, as determined by immunolabeling with antibodies to myelin basic protein (MBP) or P0 (data not shown), are significantly fewer in number in infected cultures (Fig. 4 *D* and *L*). Ultrastructural studies clearly showed that the myelin sheaths were significantly thinner in ≈60% of myelinated Schwann cells in infected cultures as compared with controls. Those LCMV-infected Schwann cells that form thick myelin sheaths (thickness of compact myelin sheath comparable to controls as in Fig. 4*G*) showed a mild form of demyelination to varying degree as indicated by the separation of myelin lamellae, but preserved axons (Fig. 4*I*). Although LCMV-NP antigens (Fig. 4*I Lower*) and viral replication (Fig. 4*L*) could be detected in these cultures, axonal ensheathment and the morphology of nonmyelinated Schwann cells and their enclosed axons were found to be normal (Fig. 4 *H* and *I*). On the other hand, in comparison to infection of immature Schwann cells, LCMV infection of mature myelinated cultures (3- to 4-week-old cultures that have already formed myelin sheaths, and the organized basal lamina) did not affect the myelin sheath or the organization of laminin-2 network.

Defective Myelination in LCMV Infection Correlates with Disorganization of Laminin-2 Network. We studied the relationship of myelination and the assembly of laminin-2/basal lamina in persistently infected LCMV cultures. Immuno-double labeling of DRG explant cultures that have myelinated for 3 weeks with antibodies specific for MBP (or P0) and laminin α2 chain showed that all myelinated nerve fibers (MBP or P0 positive) with intact myelin segments (separated by nodes of Ranvier) were colocalized with laminin α2 chain (Fig. 4 *A* and *B*). Laminin α2 not only demarcated individual myelinated nerve fibers but also expressed continuously along each myelinated fiber (Fig. 4 *A* and *B*, arrowheads). This finding suggests the presence of an organized laminin-2 network, and thus basal lamina, on each myelinated Schwann cell-axon units. In contrast, parallel cultures persistently infected with LCMV were defective in myelination and also formed a severely disorganized laminin-2 network (Fig. 4 *D* and *E*). Also, electron microscopy studies indicated that thinly formed myelin sheaths in infected Schwann cells do not have the organized basal lamina (Fig. 4 *J* and *K*). Although viral replication (Fig. 4*L*) and LCMV-NP antigen (Fig. 4*I Lower*) could be detected in infected cultures, the 4′,6-diamidino-2-phenylindole nuclear labeling (Fig. 4 *C* and *F*), and ultrastructural morphology, except myelin sheaths and basal laminae (Fig. 4 *G–K*), are indistinguishable from controls, suggesting that the defect in

Fig. 4. Persistent LCMV infection rendered immature Schwann cells defective in myelin formation: Role in laminin-2 assembly. (*A–F*) DRG explant cultures at day 5 were infected with LCMV cl-13 and allowed to differentiate in the presence of ascorbic acid, which initiate both basal lamina assembly and myelination (*D–F*). Control cultures were maintained in parallel without LCMV (*A–C*). After 21 days, both infected and control cultures were triple-labeled with anti-MBP mAb and anti-laminin α2 chain polyclonal Ab and with Hoechst dye to detect the myelination (*A* and *D*), laminin-2 organization (*B* and *E*), and nuclei (*C* and *F*), respectively. One myelinated fiber with intact myelin segments and the corresponding laminin-2 organization are shown by the arrowheads in *A* and *B*. (*G–I*) Ultrastructural analysis of LCMV-induced myelin defects. (*G*) Representative electron micrograph of uninfected explant cultures as in *A* showing Schwann cell-axon units with intact myelin sheaths (arrows) and nonmyelinated Schwann cells that enclose several axons (arrowheads). (*H*) Persistent LCMV infection causes defect in myelin sheath formation. Note the thin myelin sheaths in several Schwann cell-axon units in infected cultures (arrows). (*I*) In infected cultures, a population of Schwann cells with myelin sheaths that are normal in thickness (as in *G*) show signs of demyelination as indicated by the separation of myelin lamellae (arrows) but with intact axons (Ax). (*I Lower*) All Schwann cells in parallel cultures (as in *G–I*) are heavily infected with LCMV as detected by immunofluorescence using mAb 1-1-3 to LCMV-NP. (*J* and *K*) Ultrastructural details of the basal lamina and myelin sheath in control (*J*) and infected cultures (*K*). Representative examples showing continuos electron-dense basal lamina (BL) adjacent to the Schwann cell membrane (M), and compact myelin sheaths (MS) in control and infected explant cultures. Note the significantly thin myelin sheath as compared to control just beneath the disrupted basal lamina in infected cultures; Ax denotes the axon. (*L*) Time course analysis of persistent LCMV cl-13 infection and myelination. Quantification of MBP-positive myelin segments in control and LCMV-infected explant cultures at different time points reveals significant inhibition of overall myelination in infected cultures at each time point ($P < 0.001$). Persistent infection and viral replication in Schwann cells was confirmed by the LCMV titers (pfu/ml) from the supernatants of the same cultures at indicated time points, as well as by detection of LCMV-NP antigens with mAb 1-1-3 (*I Lower*). (Magnifications: ×40, *A–F*; ×8,500, *G–I*; ×15,500, *J* and *K*.)
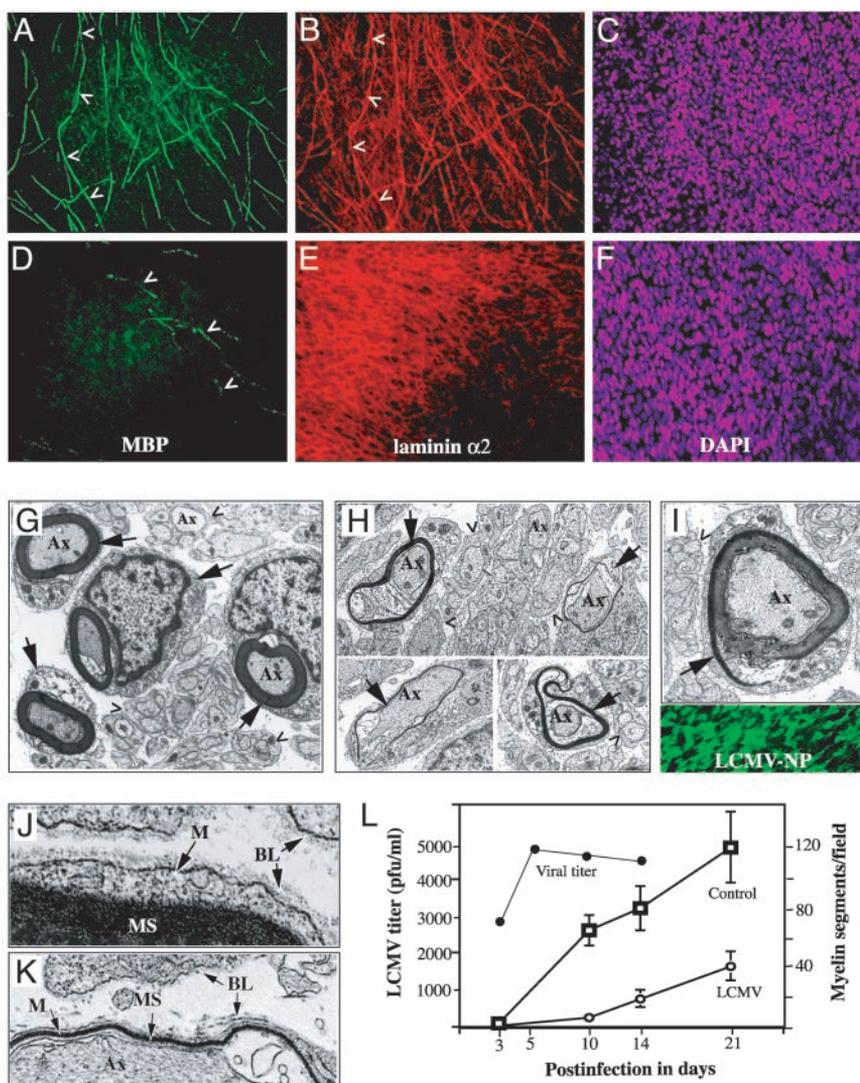
both myelination and laminin-2 assembly is not caused by apoptosis or cytopathic effects by persistent infection.

Laminin-2 Competes for LCMV Binding to Schwann Cell α-Dystroglycan. To gain further insights into the role of α-dystroglycan in LCMV-induced disorganization of the laminin-2 network on Schwann cell-axon units, we performed competitive binding assays with laminin-2 and LCMV on immobilized α-dystroglycan. Using ELISA with immobilized purified α-dystroglycan on microtiter plates, we showed that α2 laminins (a mixture of laminin-2 and laminin-4 with common tissue-restricted α2 chain) at a concentration as low as 20 nM is sufficient to block LCMV binding to α-dystroglycan, whereas fibronectin and BSA did not show any inhibitory effect (Fig. 5, which is published as supporting information on the PNAS web site). Also, LCMV binding to Schwann cell α-dystroglycan in VOPBA is competitively inhibited by α2 laminins (data not shown).

Discussion

In the present study, we identified the Schwann cell as the PNS target for LCMV and LFV and showed that this neural permissiveness is caused by the abundance of viral receptor α-dystroglycan on Schwann cells. Using an *in vitro* differentiation model of

Schwann cells, we provided evidence that LCMV ablated laminin-2–dystroglycan linkage and perturbed laminin-2 network and basal lamina assembly on mature Schwann cell-axon units. Our data indicated that these sequential events subsequently affected the myelin sheath formation when infected cells differentiated into myelinating phenotype, however, leaving nonmyelinating Schwann cells unaffected. Because defective myelination affects nerve conduction velocities and auditory functions (25, 35), congenital infection with LCMV and LFV could produce lasting neurological abnormalities in infants and children (9).

Receptor ligation by viruses during cellular entry has important functional and pathogenic consequences. However, less is known about viral ligation of cell receptors in the nervous system. As in the case with some host ligands (41), viral ligation of cell receptors may cut short receptor-associated cellular activation and functions by decreasing the level of surface receptors. Consequences of such events, particularly in immature cells, such as in the developing fetus, could be more dramatic when they differentiate to mature stage. In the present study, we showed that high-affinity binding of LCMV cl-13 to Schwann cell α-dystroglycan down-regulated its expression selectively on Schwann cell-axon units. Because α-dystroglycan down-regulation in infected cells was observed during early differentiation, it is likely that this effect started appearing

NEUROSCIENCE

before the promyelinating stage, and that the myelin defect in differentiated Schwann cells may be an indirect consequence of viral modulation of the dystroglycan complex.

The proper anchorage of laminin-2 to laminin-2 receptors on Schwann cells is believed to be critical for the self-assembly of laminin-2, which then interacts with other ECM components, such as collagen IV to form an organized basal lamina around each Schwann cell-axon unit (reviewed in refs. 25 and 27). Recent studies have shown that laminin binding/assembly on Schwann cells depends in part on the interaction of laminin with α-dystroglycan (24). Infection of immature Schwann cells by LCMV at the early stage of Schwann cell differentiation *in vitro* likely ablates laminin-2 binding to α-dystroglycan, and thus disrupts the organization of laminin-2 network and basal lamina assembly. The latter could also occur because of the lack of coordination and cross talk between dystroglycan and other laminin-2 receptors during LCMV infection. Moreover, in persistently infected cultures, LCMV-GP, in addition to LCMV virion, may also serve as a potent laminin-2 competitor for α-dystroglycan.

Increasing evidence now suggests that signaling plays crucial role in myelinogenesis (42–44). Conditional deletion of the gene for laminin-2 receptor β1 integrin in immature Schwann cells, before the formation of promyelinating Schwann cells, causes neuropathy with markedly delayed myelination (43). Similarly, more recent studies have shown that Schwann cell-specific disruption of dystroglycan gene causes significant defects in myelination in adult mice (24). These results underscore that signaling through laminin-2–laminin-2 receptors play a critical role in the differentiation of immature Schwann cells to myelinating phenotypes. Because the basal lamina has an essential role in promoting Schwann cell myelination, and the evidence from other systems shows that properly assembled laminins provide morphogenetic signals essential for epithelial development (27, 45), we propose that defective formation of myelin sheath by LCMV could be caused partly by the ablation of laminin-2–laminin-2 receptor associated signaling during differentiation of LCMV-infected immature Schwann cells to myelinating phenotypes.

Finally, the identification that LCMV and LFV use Schwann cell α-dystroglycan for peripheral nerve entry may have important implications in ill-understood Schwann cell functions associated with dystroglycan complex. Studies from genetic and functional ablation of laminin-2 and its receptors including dystroglycan provide evidence that these molecules are crucial for PNS and CNS abnormalities associated with congenital muscular dystrophy (CMD) (21, 22, 29, 30, 46). Like in gene deletion of laminin-2 and its receptors, LCMV infection disrupts α-dystroglycan–laminin linkage, a characteristic feature in CMD, and produced myelin defects. Therefore, persistent LCMV infection in Schwann cells may be a useful model to gain molecular insights into peripheral neuropathies in CMD. Although dystroglycan complex and laminin-2 appears to play a role in LCMV-induced myelin defects, we cannot exclude the possibilities of the involvement of other important mechanisms, because viruses are known to exploit multiple cellular functions for their own survival within the host. Importantly, because our understanding of the molecular basis for myelination process is limited, noncytolytic viruses such as LCMV, which can now be genetically manipulated (47), should provide an excellent model for dissecting the molecular basis of the myelination process.

1. Peters, C. J., Buchmeier, M. B., Rollin, P. E. & Ksiazek, T. G. (1996) in *Fields Virology*, eds. Fields, B. N., Knipe, D. L. & Howley, P. M. (Lippincott–Raven, Philadelphia), pp. 1505–1519.
2. Rybak, L. P. (1990) *J. Am. Med. Assoc.* **264**, 2119.
3. Cummins, D., McCormick, J. B., Bennett, D., Samba, J. A., Farrar, B., Machin, S. J. & Fisher-Hoch, S. P. (1990) *J. Am. Med. Assoc.* **264**, 2093–2096.
4. Gunther, S., Weisner, B., Roth, A., Grewing, T., Asper, M., Drosten, C., Emmerich, P., Petersen, J., Wilczek, M. & Schmitz, H. (2001) *J. Infect. Dis.* **184**, 345–349.
5. Cummins, D., Bennett, D., Fisher-Hoch, S. P., Farrar, B., Machin, S. J. & McCormick, J. B. (1992) *J. Trop. Med. Hyg.* **95**, 197–201.
6. Cole, G. A., Gilden, D. H., Monjan, A. A. & Nathanson, N. (1971) *Fed. Proc.* **30**, 1831–1841.
7. Campo, A., del Cerro, M., Foss, J. A., Ison, J. R., Orr, J. L., Warren, P. H. & Monjan, A. A. (1985) *Int. J. Neurosci.* **27**, 85–90.
8. Ormay, I. & Kovacs, P. (1989) *Orv Hetil. (Hungarian)* **130**, 789–791.
9. Barton, L. L. & Mets, M. B. (2001) *Clin. Infect. Dis.* **33**, 370–374.
10. Walker, D. H., McCormick, J. B., Johnson, K. M., Webb, P. A., Komba-Kono, G., Elliott, L. H. & Gardner, J. J. (1982) *Am. J. Pathol.* **107**, 349–356.
11. McCormick, J. B. & Fisher-Hoch, S. P. (2002) *Curr. Top. Microbiol. Immunol.* **262**, 75–109.
12. Oldstone, M. B. A. (2002) *Curr. Top. Microbiol. Immunol.* **263**, 83–118.
13. Oldstone, M. B. A., Sinha, Y. N., Blount, P., Tishon, A. I., Rodriguez, M., Von Wedel, P. & Lampert, P. W. (1984) *Science* **218**, 1125–1127.
14. Meyer, B. J., de la Torre, J. C. & Southern, P. J. (2002) *Curr. Top. Microbiol. Immunol.* **262**, 139–157.
15. Cao, W., Henry, M. D., Borrow, P., Yamada, H., Elder, J. H., Ravkov, E. V., Nichol, S. T., Compans, R. W., Campbell, K. P. & Oldstone, M. B. A. (1998) *Science* **282**, 2079–2081.
16. Sevilla, N., Kunz, S., Holz, A., Lewicke, H., Homann, D., Yamada, H., Campbell, K., de La torre, J. & Oldstone, M. B. A. (2000) *J. Exp. Med.* **192**, 1249–1260.
17. Kunz, S., Sevilla, N., Mcgavern, D., Campbell, K. & Oldstone, M. B. A. (2001) *Mol. J. Cell Biol.* **155**, 301–310.
18. Kunz, S., Borrow, P. & Oldstone, M. B. A. (2002) *Curr. Top. Microbiol. Immunol.* **262**, 111–138.
19. Ibraghimov-Beskrovnaya, O., Ervasti, J. M., Leveille, C. J., Slaughter, C. A., Sernett, S. W. & Campbell, K. P. (1992) *Nature* **355**, 696–702.
20. Yamada, H., Denzer, A., Hori, J., Tanaka, H., Anderson, L. V. B., Fujita, S., Fukutaohi, H., Shimizu, T., Ruegg, M. A. & Matsumura, K. (1996) *J. Biol. Chem.* **271**, 23418–23423.
21. Henry, M. D. & Campbell, K. P. (1998) *Cell* **95**, 859–870.
22. Colognato, H., Winkelmann, D. A. & Yurchenco, P. D. (1999) *J. Cell Biol.* **145**, 619–631.
23. Saito, F., Moore, S. A., Barresi, R., Henry, M. D., Messing, A., Ross-Barta S. E., Cohn, R. D., Willamson, R. A., Sluka, K. A., Sherman, D. L., *et al.* (2003) *Neuron* **38**, 747–758.
24. Tsiper, M. V. & Yurchenco, P. D. (2002) *J. Cell Sci.* **115**, 1005–1015.
25. Scherer S. S. & Arroyo E. J. (2002) *J. Peripher. Nerv. Syst.* **7**, 1–12.
26. Eldridge, E. F., Bunge, M. B. & Bunge, R. P. (1989) *J. Neurosci.* **9**, 625–638.
27. Bunge, M. B. (1992) in *Schwann Cell Regulation of Extracellular Matrix Biosynthesis and Assembly*, eds. Dyck, P. J., Thomas, P. K., Griffin, J., Low, P. A. & Poduslo, J. F. (Saunders, Philadelphia), pp. 299–316.
28. Leivo, I. & Engvall, E. (1988) *Proc. Natl. Acad. Sci. USA* **85**, 1544–1548.
29. Sunada, Y., Bernier, S. M., Kozak, C. A., Yamada, Y. & Campbell, K. P. (1994) *J. Biol. Chem.* **269**, 13729–13732.
30. Matsumura, K., Yamada, H., Saito, F., Sunada, Y. & Shimizu, T. (1997) *Neuromuscul. Disord.* **7**, 7–12.
31. Talts, J. F., Andac, Z., Gohring, W., Brancaccio, A. & Timpl, R. (1999) *EMBO J.* **18**, 863–870.
32. Dutko, F. J. & Oldstone, M. B. A. (1983) *J. Gen. Virol.* **64**, 1689–1698.
33. Ahmed, R., Salmi, A., Butler, L. D., Chiller, J. M. & Oldstone, M. B. A. (1984) *J. Exp. Med.* **160**, 521–540.
34. Soneoka, Y., Cannon, P., Ramsdale, E. M., Griffiths, J. C., Romano, G., Kingsman, S. M. & Kingsman, A. J. (1995) *Nucleic Acids Res.* **23**, 628–633.
35. Einheber, S., Milner, T. A., Giancotti, F. & Salzer, J. L. (1993) *J. Cell Biol.* **123**, 1223–1236.
36. Rambukkana, A., Yamada, H., Zanazzi, G., Mathus, T., Salzer, J. L., Yurchenco, P. D., Campbell, K. P. & Fischetti, V. A. (1998) *Science* **282**, 2076–2079.
37. Rambukkana, A., Zanazzi, G., Tapinos, N. & Salzer, J. L. (2002) *Science* **296**, 927–931.
38. Casella, G. T. B., Bunge, R. P. & Wood, P. (1996) *Glia* **17**, 327–338.
39. Ng, V., Zanazzi, G., Timpl, R., Talts, J. F., Salzer, J. L., Brennan, P. J. & Rambukkana, A. (2001) *Cell* **103**, 511–524.
40. Mirsky, R. & Jessen, K. R. (1999) *Brain Pathol.* **9**, 293–311.
41. Soubeyran, P., Kowanetz, K., Szymkiewicz, I., Langdon, W. Y. & Dikic, I. (2002) *Nature* **416**, 183–187.
42. Sherman, D. L., Fabrizi, C., Gillespie, C. S. & Brophy, P. J. (2001) *Neuron* **30**, 677–687.
43. Feltri, M. L., Graus Porta, D., Previtali, S. C., Nodari, A., Migliavacca, B., Cassetti, A., Littlewood-Evans, A., Reichardt, L. F., Messing, A., Quattrini, A., *et al.* (2002) *J. Cell Biol.* **156**, 199–209.
44. Scherer, S. S. (2002) *J. Cell. Biol.* **156**, 13–15.
45. Schuger, L., Yurchenco, P., Relan, N. K. & Yang Y. (1998) *Int. J. Dev. Biol.* **42**, 217–220.
46. Michele, D. E., Barresi, R., Kanagawa, M., Saito, F., Cohn, R. D., Satz, J. S., Dollar, J., Nishino, I., Kelley, R. I., Somer, H., *et al.* (2002) *Nature* **418**, 417–422.
47. Lee, K. J. & de la Torre, J. C. (2002) *Curr. Top. Microbiol. Immunol.* **262**, 175–193.